IEEE Access
Multidisciplinary | Rapid Review | Open Access Journal

Received May 15, 2020, accepted May 30, 2020, date of publication June 11, 2020, date of current version June 26, 2020.

Digital Object Identifier 10.1109/ACCESS.2020.3001876

Performance Analysis and Enhancements for In-Band Full-Duplex Wireless Local Area Networks

MURAD MURAD[1], (Member, IEEE), AND AHMED M. ELTAWIL[2], (Senior Member, IEEE)
[1]Department of Electrical Engineering and Computer Science, University of California Irvine, Irvine, CA 92697, USA
[2]Computer, Electrical, and Mathematical Science and Engineering Division, King Abdullah University of Science and Technology, Thuwal 23955, Saudi Arabia
Corresponding author: Murad Murad (mmurad@uci.edu)

ABSTRACT In-Band Full-Duplex (IBFD) is a technique that enables a wireless node to simultaneously transmit a signal and receive another on the same frequency band. Thus, IBFD wireless systems can theoretically provide up to twice the channel capacity compared to conventional Half-Duplex (HD) systems. In order to study the feasibility of IBFD networks, reliable models are needed to capture anticipated benefits of IBFD above the physical layer (PHY). In this paper, an accurate analytical model based on Discrete-Time Markov Chain (DTMC) analysis for IEEE 802.11 Distributed Coordination Function (DCF) with IBFD capabilities is proposed. The model captures all parameters necessary to calculate important performance metrics which quantify enhancements introduced as a result of IBFD solutions. Additionally, two frame aggregation schemes for Wireless Local Area Networks (WLANs) with IBFD features are proposed to increase the efficiency of data transmission. Matching analytical and simulation results with less than 1% average errors confirm that the proposed frame aggregation schemes further improve the overall throughput by up to 24% and reduce latency by up to 47% in practical IBFD-WLANs. More importantly, the results assert that IBFD transmission can only reduce latency to a suboptimal point in WLANs, but frame aggregation is necessary to minimize it. Finally, energy-efficiency is compared for both HD and IBFD networks. In comparison with the HD counterpart, IBFD systems can deliver superior energy efficiency for a given traffic scenario at the cost a higher power consumption.

INDEX TERMS In-band full-duplex, WLAN, IEEE 802.11 DCF, Markov chains, throughput, latency, frame aggregation, power consumption, energy-efficiency.

I. INTRODUCTION

The growth of video traffic led to larger data loads in the downlink (DL) direction to users as compared to uplink (UL) data from users. Even with the prevalence of social networks, where users frequently upload content, the degree of viewership of video has continued to outpace upload leading to a pattern of asymmetric data traffic that is expected to continue for the upcoming years [1]. Additionally, while Ethernet traffic is declining, WiFi traffic is growing [2]. Therefore, data traffic in Wireless Local Area Networks (WLANs) is becoming more asymmetric, and this pattern of asymmetry is expected to continue to be the norm. IEEE 802.11 standard defined in [3] enables client Stations (STAs) to communicate with an Access Point (AP). IEEE 802.11 Distributed Coordination Function (DCF) constitutes the foundation of the Medium Access Control (MAC) protocol for WLANs. By design, IEEE 802.11 DCF does not consider the amount of backlogged traffic a node has when granting access to the wireless channel. Thus, all WLAN nodes (i.e., the AP and client STAs) have an equal opportunity to access the channel despite the asymmetry between traffic loads in the UL and DL directions. Consequently, traffic asymmetry coupled with equal access to the channel leads to serving data traffic inefficiently in contemporary WLANs. As a result, there is an increasing pressure to design future wireless networks that can cope with demands for higher data rates, lower latency, and efficient utilization of resources.

Today's WLANs are Half-Duplex (HD), in that they allow either UL or DL transmission over a channel at any given time. A promising solution is to use In-Band Full-Duplex (IBFD) technique in order to make an efficient use of

The associate editor coordinating the review of this manuscript and approving it for publication was Xijun Wang.

available network resources. IBFD communications, enabled by Self-Interference Cancellation (SIC) solutions, can theoretically double channel capacity by allowing each wireless node to transmit and receive at the same time and over the same frequency band (see [4], [5], or [6] for a comprehensive coverage of IBFD communications).

Prior advancements in SIC affirm that IBFD is possible, and the legacy assumption of a single transmission over a frequency is no longer a necessity. SIC can be implemented at different levels and in numerous ways. A possible SIC solution can take place in the analog domain at both the transmitter and receiver sides [7]. On the other hand, SIC can be treated in the digital domain at the transceiver as in [8]. An innovative method can extract the Self-Interference (SI) signal from the analog domain and cancel it at the digital domain as in [9]. Alternatively, the SI signal can be extracted from the digital domain and canceled at the analog domain to enable proper reception for the Signal of Interest (SOI) [10]. A combination of SIC techniques at various levels is often necessary to reduce SI below the noise floor in order to maximize the Signal to Interference and Noise Ratio (SINR) of the SOI. As a result, several platforms utilizing IEEE 802.11 standard are already operational as IBFD-WLANs (see [11], [12], and [13] as examples). This paper assumes perfect SIC and goes beyond PHY-layer analysis to provide essential contributions at the MAC-sublayer.

A. MAIN CONTRIBUTIONS

The contributions of this paper are summarized as follows:

- An accurate analytical model is constructed based on Discrete-Time Markov Chain (DTMC) analysis to calculate throughput, latency, and energy-efficiency for IBFD-WLANs. The average error of the analytical model in this paper is less than 1% compared with up to 13% from a prior model as illustrated in this paper's results.
- Two distributed frame aggregation solutions for IBFD-WLANs are proposed to serve data traffic efficiently. Throughput is improved by up to 24% and latency is reduced by up to 47% in IBFD-WLANs.
- Numerical performance metrics are formalized in order to address performance limits and enhancements due to employing IBFD in WLANs.

In the proposed aggregation schemes, each STA can make an independent decision about the possibility and amount of aggregation based on knowing the size of the traffic it receives. Matching analytical and simulation results indicate that IBFD aggregation yields a maximum system throughput. While increasing the size of data traffic intuitively leads to increased network throughput, latency analysis and simulation in this paper emphasize that aggregation is a necessary condition to reduce the average delay of frame delivery. Furthermore, while implementing IBFD generally increases power consumption due to the increase in transmission and receiving activities at each wireless node, the results presented in this paper confirm that IBFD increases energy-efficiency in WLANs. Fig. 1 illustrates a typical IBFD-WLAN with asymmetric traffic loads and the potential of frame aggregation. Since STAs always have smaller UL frames, aggregation is possible by combining multiple frames if they can fit within the available DL longer duration.

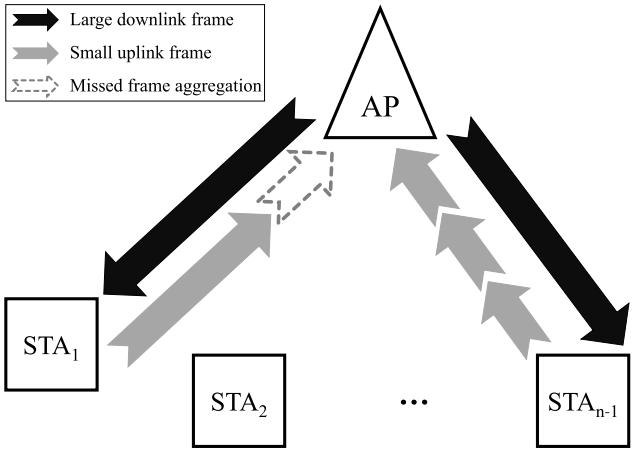

FIGURE 1. A typical IBFD-WLAN with asymmetric traffic loads.

B. PAPER ORGANIZATION

The rest of this paper is organized as follows. Section II gives a summary of prior work. Section III provides an overview of the technical background necessary to establish the HD IEEE 802.11 reference model. Section IV outlines the system model and operational scenario of the work. Section V details the proposed analytical model for IBFD-WLAN. Section VI establishes performance metrics and explains the proposed IBFD aggregation schemes. Section VII describes the discrete-event simulator built to model typical WLANs. Section VIII illustrates the generated results. The paper is then concluded in Section IX.

II. RELATED WORK

There were several previously published research attempts to provide analytical models for IBFD MAC protocols. Some deficiencies in existing literature include:

- **Deviation from IEEE 802.11 standard:** in [14], a MAC protocol for wireless ad hoc networks is studied based on a three-dimensional DTMC model, but the proposed protocol deviates from IEEE 802.11 DCF mechanism and neglects to derive IBFD-compatible expressions for the probability of transmission. The two-dimensional DTMC model outlined in [15] does not account for starting a new contention cycle after a node successfully gets an IBFD transmission opportunity, and the model does not follow IEEE 802.11 when it comes to an unsuccessful transmission at the maximum backoff stage. An Embedded Markov Chain model is used in [16] to study a Carrier-Sense Multiple Access with

Collision Avoidance (CSMA/CA) MAC protocol, but the proposed protocol uses a fixed contention window and does not follow IEEE 802.11 Binary Exponential Backoff in case of a collision.

- **Limited IBFD considerations:** the IBFD MAC protocol in [17] focuses on simultaneous transmitting and sensing, but the analysis does not fully exploit IBFD benefits for increasing throughput and reducing latency. The authors of [18] model a new MAC protocol as a three-dimensional DTMC to use IBFD-synchronized transmission only after a successful HD transmission, but the model does not treat collisions accurately.
- **Impractical network topology:** while [19] addresses both throughput and delay in the three-dimensional DTMC analysis for a proposed distributed MAC protocol, the work primarily focuses on multi-hop networks.
- **Incomplete analytical expressions:** the IBFD MAC protocol proposed in [20] limits IBFD capabilities to the AP only and substantially neglects to show the details of the theoretical work leading to a basic expression for the probability of transmission.
- **Inaccurate results:** the reported results for throughput and delay in [21] show a major mismatch between theoretical and simulation results. Both inaccuracy of results and lack of a full model for IBFD-WLANs are resolved in this paper.
- **Different analytical approaches:** IBFD-WLAN analytical models should extend from existing HD IEEE 802.11 analysis (i.e., based on well-established models like [22]). The work in this paper substantially differs from the Renewal Theory approach described in [23], which quantifies and expresses probability values differently. The model in [23] also diverts from establishing the values of some system parameters according to the IEEE 802.11 standard and does not provide insight on latency. The approach in [24] uses two separate Markov Chains while this paper uses a two-dimensional Markov Chain model in consistence with the HD model presented in [22] for ease of extension. The primary contribution in [24] is limited to considering hidden nodes for throughput while full details for analytical IBFD throughput, latency, and power consumption are provided in this paper. Additionally, no comparison with HD IEEE 802.11 is presented in [24], and the assumed parameters are based on legacy IEEE 802.11a while the current IEEE 802.11ac [25] release is assumed in this paper.
- **Complex aggregation:** the authors of [26] introduce frame aggregation in an IBFD network, but a 2-step optimization solver is needed to determine the size of the aggregated frame. Additionally, [26] assumes DCF with RTS/CTS protocol, which is unnecessary since IBFD mitigates the hidden terminal problem [13].
- **Lack of analytical models:** while references [27]–[31] all address IBFD MAC solutions, none of them provide a full analytical expression for the probability of transmission, which is a substantial part of this paper's contributions.
- **Different Focus:** some papers consider the same constraints as the ones considered in this paper such as IBFD MAC, WLANs, and asymmetric traffic. However, the focus of this paper is on accurately modeling IBFD-WLANs analytically, which is different from, for example, [32] which focuses on QoS.

TABLE 1. Key symbols and corresponding terms.

Symbol	Description of Term
τ	Probability of transmitting
p	Conditional collision probability
W	Initial Contention Window
R	Maximum number of re-transmission attempts
n	Total number of nodes
P_s	Probability of a successful transmission
P_{tr}	Probability there is at least a transmission
$\overline{E[P]}$	Expected payload size
$\overline{T_s}$	Expected time needed for a successful transmission
$\overline{T_c}$	Expected time spent during a collision
σ	Time slot duration
SIFS	Short Interframe Space
DIFS	DCF Interframe Space
ACK	Acknowledgment frame
m	Maximum backoff stage
ρ	Symmetry Ratio for each node
Φ	Full-Duplex Factor for the system
β	Probability of reply-back IBFD transmission
α	Probability of not getting reply-back IBFD transmission
γ	IBFD aggregation factor for each node
η	IBFD link utilization for the system
S	System throughput
D	End-to-end latency
$\mathcal{E}$	Energy consumption per node
ω	Power consumption per node

III. TECHNICAL BACKGROUND ON HD IEEE 802.11 DCF

TABLE 1 describes key symbols and terms used throughout the paper. A well-celebrated analytical model for IEEE 802.11 DCF was presented in [22]. This model was subsequently revised a number of times, especially when it comes to the *probability of transmitting* (τ). To provide a reference base for HD IEEE 802.11 DCF, τ is adopted from the refined model published in [33] as

$$\tau = \frac{1}{1 + \frac{1-p}{1-p^{R+1}} \sum_{i=0}^{R} p^i (2^i W - 1)/2 - \frac{1-p}{2}} \tag{1}$$

where W is the initial Contention Window ($\mathrm{CW}_{\min}$), R is the maximum number of re-transmission attempts, and p is the *conditional collision probability*. An STA experiences a collision when at least one other wireless node concurrently transmits. Therefore,

$$p = 1 - (1 - \tau)^{n-1} \tag{2}$$

where n is the total number of nodes. Equations (1) and (2) can simply be solved numerically to calculate the values of τ and p for each node.

The *probability of a successful transmission* (P_s) is the conditional probability of having exactly one transmission

given that there is at least one transmission. Accordingly, (P_s) is given by

$$P_s = \frac{n\tau(1-\tau)^{n-1}}{1-(1-\tau)^n}. \tag{3}$$

The *throughput* (S) in bits per second (bps) is calculated as

$$S = \frac{P_s P_{tr} \overline{E[P]}}{(1-P_{tr})\sigma + P_{tr}P_s\overline{T_s} + P_{tr}(1-P_s)\overline{T_c}} \tag{4}$$

where P_{tr} is the *probability that there is at least a transmission*, and it is given by

$$P_{tr} = 1-(1-\tau)^n. \tag{5}$$

According to [33], an accurate characterization for the throughput is achieved if the *expected payload size* $\overline{E[P]}$, the *expected time needed for a successful transmission* ($\overline{T_s}$), and the *expected time spent during a collision* ($\overline{T_c}$) are respectively expressed as

$$\overline{E[P]} = P\frac{W}{W-1}, \tag{6}$$

$$\overline{T_s} = T_s\frac{W}{W-1} + \sigma, \tag{7}$$

and

$$\overline{T_c} = T_c + \sigma, \tag{8}$$

where

$$T_s = \text{H} + \text{payload time} + \text{SIFS} + \text{ACK} + \text{DIFS}, \tag{9}$$

$$T_c = \text{H} + \text{collision time} + \text{SIFS} + \text{ACK} + \text{DIFS}, \tag{10}$$

P is the payload size in bits, and H is the total time for both PHY and MAC headers. Values for headers, SIFS, ACK, DIFS, and time slot duration (σ) are set by IEEE 802.11 standard. TABLE 2 shows the values of PHY and MAC parameters based on the IEEE 802.11ac release [25].

TABLE 2. IEEE 802.11ac PHY/MAC selected parameters.

Parameter	Value
Frequency	5 GHz band
Channel bandwidth	80 MHz
Modulation scheme	16-QAM
Code rate	1/2
Spatial streams	2×2 MIMO
PHY header duration	44 μs
Guard Interval	800 ns
Data rate (UL and DL)	234 Mbps
Basic rate	24 Mbps
MAC header size	36 bytes
FCS size	4 bytes
ACK size	14 bytes
MPDU_{max} size	7,991 bytes
Slot duration (σ)	9 μs
SIFS duration	16 μs
DIFS duration	34 μs
CW_{min}	16
CW_{max}	1024

Considering the system model detailed in the next section, analytical expressions for the expected size of successfully transmitted MAC Protocol Data Unit (MPDU) and the expected size of a collision are thoroughly derived in [34] and can respectively be simplified as

$$(E[P])^{HD} = \frac{n+1}{2n}\cdot \text{MPDU}_{\text{max}} \tag{11}$$

and

$$(E[P^*])^{HD} \approx \left[\frac{0.3519\times\tau(1-(1-\tau)^{n-1})}{1-(1-\tau)^{\text{n-n}}\tau(1-\tau)^{n-1}} + 0.6481\right] \times \text{MPDU}_{\text{max}}. \tag{12}$$

Latency is calculated as the average time from the instant a frame becomes Head-of-Line (HOL) until the frame is successfully delivered. The analytical expression for latency in HD IEEE 802.11 is derived in [35] directly from the well-known Little's Theorem (see [36] for further explanation) as

$$D = \frac{n}{S/E[P]}. \tag{13}$$

Power consumption is based on the classical definition of power [37]

$$\text{Power} \triangleq \frac{\text{Energy}}{\text{Time}}. \tag{14}$$

As presented in [38], the energy consumed by a node in an HD WLAN depends on the state of the node. There are six mutually exclusive states a node can be in. The energy consumption ($\mathcal{E}$) in terms of power consumption (ω) and the probability for each state are given as follows

1) Idle (d) state

$$\mathcal{E}_{\text{d}} = \omega_{\text{d}}\sigma \tag{15}$$

$$Pr(\text{d}) = (1-\tau)^n \tag{16}$$

2) Successful transmission (S-TX) state

$$\mathcal{E}_{\text{S-TX}} = \omega_{\text{TX+CTRL}}\text{DATA}_{\text{TX}} + \omega_{\text{d}}(\text{DIFS}+\text{SIFS}) + \omega_{\text{RX+CTRL}}\text{ACK} \tag{17}$$

$$Pr(\text{S-TX}) = \tau(1-p) \tag{18}$$

3) Successful reception (S-RX) state

$$\mathcal{E}_{\text{S-RX}} = \omega_{\text{RX+CTRL}}\text{DATA}_{\text{RX}} + \omega_{\text{d}}(\text{DIFS}+\text{SIFS}) + \omega_{\text{TX+CTRL}}\text{ACK} \tag{19}$$

$$Pr(\text{S-RX}) = \tau(1-\tau)^{n-1} \tag{20}$$

4) Successful overhearing (S-$\overline{\text{RX}}$) state

$$\mathcal{E}_{\text{S-}\overline{\text{RX}}} = \omega_{\text{RX+CTRL}}(\text{DATA}_{\text{RX}} + \text{ACK}) + \omega_{\text{d}}(\text{DIFS}+\text{SIFS}) \tag{21}$$

$$Pr(\text{S-RX}) = (n-2)\tau(1-\tau)^{n-1} \tag{22}$$

5) Transmitting during a collision (C-TX) state

$$\mathcal{E}_{\text{C-TX}} = \omega_{\text{TX+CTRL}}\text{DATA}_{\text{TX}} + \omega_{\text{d}}(\text{DIFS}+\text{SIFS}+\text{ACK}) \tag{23}$$

$$Pr(\text{C-TX}) = \tau p \tag{24}$$

6) Overhearing a collision (C-$\overline{\text{RX}}$) state

$$\mathcal{E}_{\text{C-RX}} = \omega_{\text{RX+CTRL}}\text{DATA}_{\text{RX}} + \omega_{\text{d}}(\text{DIFS} + \text{SIFS} + \text{ACK}) \quad (25)$$

$$Pr(\text{C-}\overline{\text{RX}}) = (1-\tau)[1-(1-\tau)^{n-1} - (n-1)\tau(1-\tau)^{n-2}]. \quad (26)$$

The expected value of consumed energy by a node can be expressed in terms of the energy consumption and probability of each state as

$$E[\text{energy}] = \sum_{i=1}^{6}(\text{energy in state } i)\cdot Pr(\text{state } i). \quad (27)$$

Finally, the average power consumption of a node is given by rewriting (14) as

$$\text{Power} = \frac{E[\text{energy}]}{E[\text{time duration}]} = \frac{\sum_{i=1}^{6}(\text{energy in state } i)\cdot Pr(\text{state } i)}{(1-P_{tr})\sigma + P_{tr}P_sT_s + P_{tr}(1-P_s)T_c}. \quad (28)$$

IV. SYSTEM MODEL AND OPERATIONAL SCENARIO

This paper assumes a WLAN with an AP and $n-1$ client STAs using IEEE 802.11ac standard to communicate over a single channel. The basic mode of DCF without Request to Send/Clear to Send (RTS/CTS) handshake is assumed. In case of a collision, total frame loss occurs (no capture effect). Error-free PHY transmission is assumed, which is a common assumption in many MAC-level papers including the prominent work in [22] and its refinement in [33]. All nodes can detect one another, and the effect of hidden terminals is not considered since IBFD substantially reduces this problem [13]. Both UL and DL transmissions have the same data rate. The AP always has a load of MPDU_{max}, and there is always a frame on standby for every client STA. A saturated buffer at each node is assumed (i.e., there is always traffic to transmit). While this assumption may not reflect the traffic pattern of a typical residential WLAN, it outlines the upper performance limits of a fully congested network. Frame aggregation is possible by combining more than one MPDU to make a larger aggregated MPDU. Client STAs have Symmetry Ratio (SR) values where the value of SR at STA_i, indicated here as ρ_i, is defined in [39] as the ratio of the UL load over the DL load. If the traffic load is designated as (L) and transmission time as (T), then ρ is

$$\rho \triangleq \frac{L_{UL}}{L_{DL}} = \frac{T_{UL}}{T_{DL}}. \quad (29)$$

Each STA_i has $0.1 \leq \rho_i \leq 0.9$. STAs keep their original ρ values constant throughout each simulation run. While this traffic scenario is generic, it covers the full range of UL/DL traffic symmetry from low (i.e., $\rho = 0.1$) to high (i.e., $\rho = 0.9$).

In IBFD-WLAN scenarios, all transmissions occur as IBFD between the AP and an STA. The Full-Duplex Factor (FDF) defined in [34] as the average of all ρ values of the client STAs in the network can be calculated as

$$\Phi \triangleq \frac{\sum_{i=1}^{n-1}\rho_i}{n-1} \quad (30)$$

where $\Phi = 0$ for HD WLAN system.

Given the traffic assumptions in this paper, no additional latency overhead needs to be introduced in IBFD DCF mechanisms. When the AP gains access to the channel, it establishes a link with one of the client STAs with a probability equal to $1/(n-1)$. The client STA can immediately start transmitting since it would only be communicating with the AP. Clearly, the higher the number of client STAs, the less chance each STA has to connect to the AP. This consequently introduces fairness issues in terms of allowing the AP more chances to transmit than any one client STA since the AP also gets opportunities to transmit back due to the IBFD transmission mode whenever any STA transmits. However, this mechanism also results in improving the overall performance of the system throughput since the AP has a larger traffic load than any STA in the network as already established in the assumptions for this paper. Also, the duration of the active DL transmission from the AP is sufficient to contain the smaller UL transmission from a client STA. Even when a client STA initiates the transmission, the AP has a standby frame for every STA and does not need to stay silent. Accounting for the assumption that the AP needs to wait until it decodes the transmitting STA's address would add a negligible amount of overhead due to the much larger payload size at the AP (16 bytes from the header compared to a load of 7,991 bytes). The system-level analyses presented in this paper do not require accounting for this slight increase in latency. If the header size increases by changing the frame structure to serve special IBFD features like in [18], [27], and [40], then careful consideration for the header is necessary. However, this paper introduces no changes in any frame format.

Since UL $<$ DL, the active STA can synchronize the transmission of its ACK frame concurrently with the ACK frame of the AP at the end of the DL transmission. The ACK frames are immune from collisions since transmitting nodes only need to wait for SIFS to send ACK frames while starting a new transmission by other nodes must be delayed by the longer DIFS according to IEEE 802.11 standard.

V. ANALYTICAL MODEL FOR IBFD-WLAN

Prior works modeling contemporary IEEE 802.11 DCF were based on the assumption that all transmission takes place in a Time-Division Duplexing (TDD) fashion, which is an HD scheme. Therefore, the prominent model originally presented in [22] is no longer valid when the transmission is IBFD. In HD systems, two key parameters, namely the probability of transmitting (τ) and the conditional collision probability (p), determine the performance of a WLAN at the MAC sublayer. However, when the system is IBFD, both τ and p must be revised. First, unlike the HD case where AP and STAs share equal τ and p values, there are τ_{AP}, τ_{STA}, p_{AP}, and p_{STA} values in an IBFD network. Second, in addition to

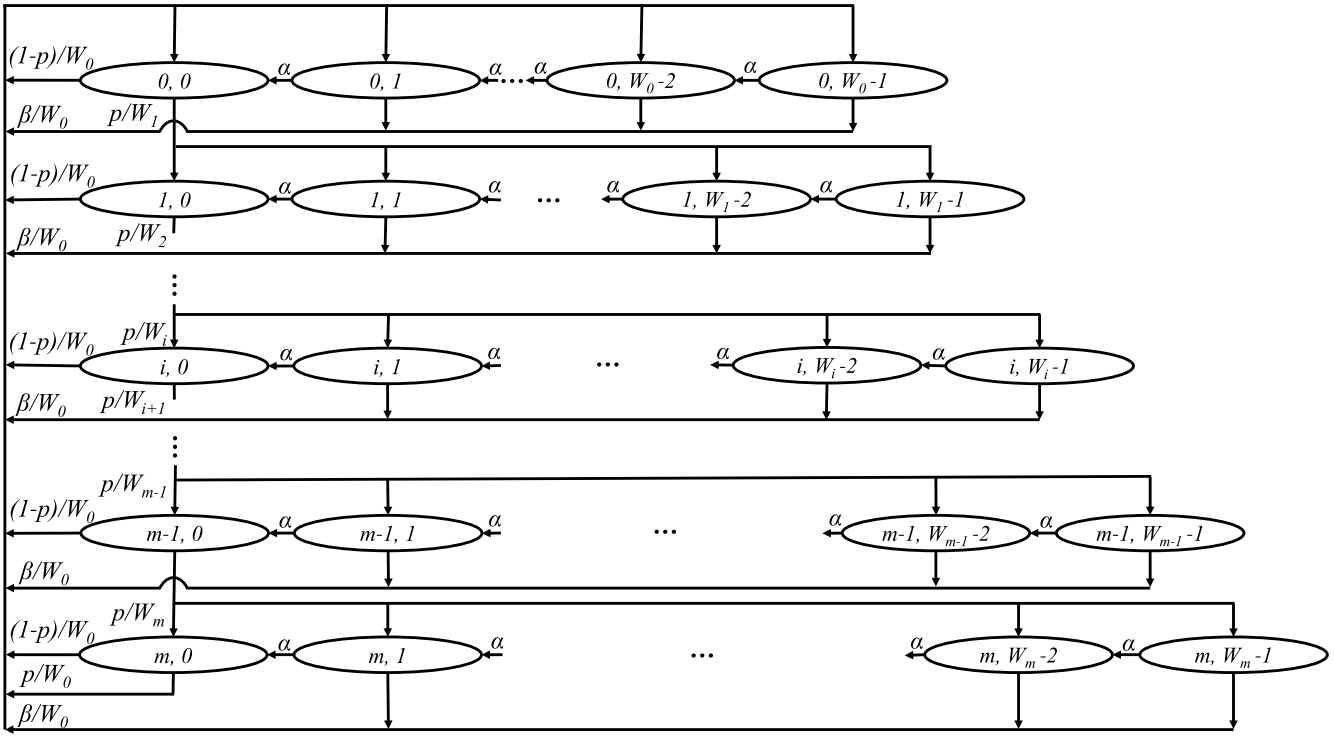

FIGURE 2. Two-dimensional DTMC representing backoff stage and backoff counter for each wireless node.

the *direct* transmission probability, τ, which happens when a node wins the contention for the channel, there is potential for IBFD *reply-back* transmission when the node is not in direct transmission ($\overline{\tau}$). The probability of reply-back transmission (β) for a tagged node happens when another node is in direct transmission with the tagged node. Third, collisions are treated differently for IBFD systems compared to a contemporary HD WLAN, which is thoroughly explained in the related conference paper [34].

While both the HD-based model in [22] and the one constructed in this paper are based on two-dimensional DTMC analyses, there are several important differences which make the proposed model here more complex. For example, when a tagged STA selects a random backoff counter other than zero in [22], the STA decrements its backoff counter with probability 1 whenever the channel is idle. On the other hand, this probability is no longer 1 when IBFD is assumed, and it is assigned a variable α as in (34) below. Additionally, since the model in [22] has only one possibility of transmission (i.e., τ), it is necessary to introduce a probability of reply-back IBFD transmission (β) at each state with backoff counter other than zero as in (35). Introducing α and β makes the DTMC analysis more complicated in the case of IBFD-WLAN model. Finally, unlike [22], thorough and systematic derivations for the stationary distribution equations are detailed in this paper to enable future enhancements for IBFD-WLANs.

In this section, analytical work is carried out to construct a model for IBFD-WLAN based on IEEE 802.11 DCF protocol. Key parameters needed to calculate important performance metrics are defined. All parameters take into account IBFD and its effects on the behavior of wireless nodes at MAC-level operations.

A. REVISED PROBABILITY OF TRANSMISSION (τ)

Fig. 2 shows the model adopted for IBFD-WLAN. The two-dimensional DTMC model represents each state in terms of backoff stage, i, and backoff counter, k. Unlike [21], the model in Fig. 2 resets its backoff stage to zero if a frame experiences a collision while the transmitting node is at the maximum backoff stage m.

The transition probabilities for the DTMC model are as follows

$$P\{0, k_0|i, 0\} = \frac{1-p}{W_0} \quad i \in [0, m-1],\ k_0 \in [0, W_0 - 1] \tag{31}$$

$$P\{i, k|i-1, 0\} = \frac{p}{W_i} \quad i \in [1, m],\ k \in [0, W_i - 1] \tag{32}$$

$$P\{0, k_0|m, 0\} = \frac{1}{W_0} \quad k_0 \in [0, W_0 - 1] \tag{33}$$

$$P\{i, k-1|i, k\} = \alpha \quad i \in [0, m], \quad k \in [1, W_i - 1] \tag{34}$$

$$P\{0, k_0|i, k\} = \frac{\beta}{W_0} \quad i \in [0, m],\ k \in [1, W_i - 1],\ k_0 \in [0, W_0 - 1]. \tag{35}$$

The stationary distribution of the chain is represented as

$$b_{i,k} \triangleq \lim_{t\to\infty} P\{s(t)=i, b(t)=k\} \quad i\in[0,m], \quad k\in[0,W_i-1] \tag{36}$$

where $s(t)$ and $b(t)$ are respectively the stochastic processes for the backoff stage and backoff counter as in [22].

Direct transmission happens when a node is at any of the possible $b_{i,0}$ states. Therefore, the probability of direct transmission is

$$\tau \triangleq \sum_{i=0}^{m} b_{i,0}. \tag{37}$$

By applying the normalization condition, the following result can be directly obtained

$$\begin{aligned} 1 &= \sum_{i=0}^{m}\sum_{k=0}^{W_i-1} b_{i,k} = \sum_{i=0}^{m} b_{i,0} + \sum_{i=0}^{m}\sum_{k=1}^{W_i-1} b_{i,k} \\ &= \tau + \sum_{i=0}^{m}\sum_{k=1}^{W_i-1} b_{i,k} \\ &\Rightarrow \overline{\tau} \triangleq 1-\tau = \sum_{i=0}^{m}\sum_{k=1}^{W_i-1} b_{i,k} \end{aligned} \tag{38}$$

where $\overline{\tau}$ is the probability that a node is not transmitting *directly*, which makes the node in a state there is potential for an *indirect* IBFD reply-back transmission if it receives data.

Calculating the expressions for both $b_{i,0}$ and $b_{0,0}$ follows. First, $b_{1,0}$ in terms of $b_{0,0}$ based on Fig. 2 is written as

$$\begin{aligned} b_{1,0} &= b_{0,0}\frac{p}{W_1} + b_{1,1}\cdot\alpha \\ &= b_{0,0}\frac{p}{W_1} + \alpha\cdot(b_{0,0}\frac{p}{W_1} + \alpha\cdot b_{1,2}) \\ &= b_{0,0}\frac{p}{W_1} + \alpha\cdot b_{0,0}\frac{p}{W_1} + \alpha^2\cdot b_{1,2} \\ &= b_{0,0}\frac{p}{W_1}(1+\alpha+\alpha^2+\ldots+\alpha^{W_1-2}) + \alpha^{W_1-1}\cdot b_{1,W_1-1} \\ &= b_{0,0}\frac{p}{W_1}(1+\alpha+\alpha^2+\ldots+\alpha^{W_1-2}) + \alpha^{W_1-1}\cdot b_{0,0}\frac{p}{W_1} \\ &= \frac{b_{0,0}\cdot p}{W_1}\sum_{j_1=0}^{W_1-1}\alpha^{j_1} \\ &= \frac{b_{0,0}\cdot p}{W_1}\cdot\frac{1-\alpha^{W_1}}{1-\alpha} \end{aligned} \tag{39}$$

based on resolving the sum of the geometric series. Similarly, calculate $b_{2,0}$ and substitute for $b_{1,0}$ from (39)

$$\begin{aligned} b_{2,0} &= \frac{b_{1,0}\cdot p}{W_2}\sum_{j_2=0}^{W_2-1}\alpha^{j_2} = \frac{b_{0,0}\cdot p}{W_1}\cdot\frac{1-\alpha^{W_1}}{1-\alpha}\cdot\frac{p}{W_2}\cdot\frac{1-\alpha^{W_2}}{1-\alpha} \\ &= \frac{b_{0,0}\cdot p^2}{W_1\cdot W_2}\cdot\frac{(1-\alpha^{W_1})(1-\alpha^{W_2})}{(1-\alpha)^2}. \end{aligned} \tag{40}$$

Noticing the pattern in $b_{1,0}$ and $b_{2,0}$, $b_{i,0}$ can be written as

$$b_{i,0} = b_{0,0}(\frac{p}{1-\alpha})^i\prod_{j=1}^{i}\frac{1-\alpha^{W_j}}{W_j}, \quad 1\le i\le m. \tag{41}$$

For $b_{0,0}$, it can directly be deduced from Fig. 2 that

$$\begin{aligned} b_{0,0} &= \sum_{i=0}^{m} b_{i,0}\cdot(1-p)\cdot\frac{1}{W_0} + \sum_{i=0}^{m}\sum_{k=1}^{W_i-1} b_{i,k}\cdot\beta\cdot\frac{1}{W_0} \\ &\quad + b_{m,0}\cdot p\cdot\frac{1}{W_0} + \alpha\cdot b_{0,1} \\ &= \tau\cdot(1-p)\cdot\frac{1}{W_0} + (1-\tau)\cdot\beta\cdot\frac{1}{W_0} \\ &\quad + b_{m,0}\cdot p\cdot\frac{1}{W_0} + \alpha\cdot b_{0,1} \\ &= \underbrace{\frac{\tau(\alpha-p)+1-\alpha+p\cdot b_{m,0}}{W_0}}_{Z} + \alpha\cdot b_{0,1} \\ &= Z + \alpha\cdot(Z+\alpha\cdot b_{0,2}) = Z(1+\alpha)+\alpha^2\cdot b_{0,2} \\ &= Z(1+\alpha+\alpha^2+\ldots+\alpha^{W_0-2}) + \alpha^{W_0-1}\cdot\underbrace{b_{0,W_0-1}}_{Z} \\ &= Z\sum_{j=0}^{W_0-1}\alpha^j = Z\cdot\frac{1-\alpha^{W_0}}{1-\alpha} \\ &= \frac{1-\alpha^{W_0}}{1-\alpha}\frac{\alpha-p}{W_0}\cdot\tau + \frac{1-\alpha^{W_0}}{W_0} + \frac{1-\alpha^{W_0}}{1-\alpha}\frac{p\cdot b_{m,0}}{W_0}. \end{aligned} \tag{42}$$

By substituting the expression for $b_{m,0}$ from (41) in (42), $b_{0,0}$ becomes

$$\begin{aligned} b_{0,0} &= \frac{1-\alpha^{W_0}}{W_0}\left[\frac{\alpha-p}{1-\alpha}\cdot\tau+1\right] \\ &\quad + \frac{1-\alpha^{W_0}}{(1-\alpha)W_0}\cdot p\cdot b_{0,0}(\frac{p}{1-\alpha})^m\prod_{j=1}^{m}\frac{1-\alpha^{W_j}}{W_j} \\ &= \frac{\frac{1-\alpha^{W_0}}{W_0}\left[\frac{\alpha-p}{1-\alpha}\cdot\tau+1\right]}{1-(\frac{p}{1-\alpha})^{m+1}\prod_{j=0}^{m}\frac{1-\alpha^{W_j}}{W_j}}. \end{aligned} \tag{43}$$

Thus, τ is readily calculated as

$$\begin{aligned} \tau &= \sum_{i=0}^{m} b_{i,0} = b_{0,0} + \sum_{i=1}^{m} b_{i,0} \\ &= b_{0,0}\left[1+\sum_{i=1}^{m}(\frac{p}{1-\alpha})^i\prod_{j=1}^{i}\frac{1-\alpha^{W_j}}{W_j}\right]. \end{aligned} \tag{44}$$

Noting that derivation of α and p is provided in the next two sub-sections, the value of τ can be numerically calculated using (43) and (44). While τ is the same for the AP and STAs in contemporary HD IEEE 802.11 DCF, its value in an IBFD-WLAN is different depending on if the transmitting node is the AP or an STA. τ_{AP} and τ_{STA} are calculated based on the corresponding α_{AP}, p_{AP}, α_{STA}, and p_{STA} values. Finally, *the average probability of transmission in the network* follows directly from the law of total probability as

$$\tau^{IBFD} = \frac{1}{n}\tau_{AP} + \frac{n-1}{n}\tau_{STA}. \tag{45}$$

B. PROBABILITY OF REPLY-BACK IBFD TRANSMISSION (β)

In IBFD-WLAN, each node has an opportunity for indirect transmission. Whenever a node is not in any of the states represented by τ, the node can have the opportunity to transmit if another node is transmitting to it. There are two cases for this to happen as follows

1) When the AP is silent, it initiates transmission whenever an STA is transmitting. This probability can be represented as

$$\begin{aligned}\beta_{AP} &= (n-1)\tau_{STA}(1-\tau_{STA})^{n-2} \\ &= (n-1)\tau_{STA}(\overline{\tau}_{STA})^{n-2}. \end{aligned} \tag{46}$$

2) When an STA is silent, it initiates transmission whenever the AP is transmitting to that particular STA. This probability is represented as

$$\begin{aligned}\beta_{STA} &= \frac{\tau_{AP}(1-\tau_{STA})^{n-2}}{n-1} \\ &= \frac{\tau_{AP}(\overline{\tau}_{STA})^{n-2}}{n-1}. \end{aligned} \tag{47}$$

For the special case when $n = 2$, (46) and (47) respectively become $\beta_{AP} = \tau_{STA}$ and $\beta_{STA} = \tau_{AP}$, which is compatible with the intuition that the AP has a reply-back opportunity whenever the STA is transmitting and vice versa. Also, based on Fig. 2, the following equation can be used to calculate both α_{AP} and α_{STA} according to the corresponding β_{AP} and β_{STA} values

$$\alpha = 1 - \beta. \tag{48}$$

where α is the probability of decreasing the backoff counter by 1 (i.e., not getting an opportunity for a reply-back transmission).

C. REVISED CONDITIONAL COLLISION PROBABILITY (p)

In HD IEEE 802.11 networks, collisions are treated in the same way for the AP and all STAs. As a result, conditional collision probability, p, is defined in [22] as previously stated (see (2) in section III). However, in IBFD scenarios, the conditional collision probability for the AP (p_{AP}) is different from that of an STA (p_{STA}). For the AP, collision-free transmission happens in either of the following two cases

1) The AP is in direct transmission while all STAs are silent.
2) The AP is in direct transmission with a tagged STA, and this tagged STA is directly transmitting back to the AP while all other STAs are silent.

Therefore, the conditional collision probability for the AP can be expressed as

$$\begin{aligned}p_{AP} &= 1 - \left[(1-\tau_{STA})^{n-1} + \tau_{STA}(1-\tau_{STA})^{n-2}\right] \\ &= 1 - \left[(\overline{\tau}_{STA})^{n-1} + \tau_{STA}(\overline{\tau}_{STA})^{n-2}\right]. \end{aligned} \tag{49}$$

For the conditional collision probability of an active STA, transmission without collision takes place when either one of the below scenarios is true

1) The AP is silent, and so are all other STAs.
2) The AP is directly transmitting back to the active STA while all other STAs are silent.

Consequently, the conditional collision probability of a tagged STA is given by

$$\begin{aligned}p_{STA} &= 1 - \left[(1-\tau_{AP})(1-\tau_{STA})^{n-2} + \frac{\tau_{AP}(1-\tau_{STA})^{n-2}}{n-1}\right] \\ &= 1 - \left[\overline{\tau}_{AP}(\overline{\tau}_{STA})^{n-2} + \frac{\tau_{AP}(\overline{\tau}_{STA})^{n-2}}{n-1}\right]. \end{aligned} \tag{50}$$

Similar to how it was detailed in [34] with simplified assumptions regarding τ, (49) and (50) indicate that a collision-free mode of IBFD transmission is achieved when $n = 2$ since both equations respectively evaluate to $p_{AP} = 0$ and $p_{STA} = 0$. When $n > 2$, both UL and DL loads are successfully transmitted when the AP and the corresponding STA are transmitting since the AP always has a frame for every STA and vice versa.

D. REVISED PROBABILITY OF SUCCESSFUL TRANSMISSION (P_s)

The probability of successful transmission for an IBFD-WLAN, P_s^{IBFD}, happens during any one of the following four conditional probabilities

1) There is exactly one direct transmission by the AP and all STAs are silent given there is at least a direct transmission.
2) There is exactly one direct transmission by an STA while the AP and all other STAs are silent given there is at least a direct transmission.
3) There are exactly two direct transmissions; one is by the AP and the other is by the corresponding STA back to the AP given that there is at least a direct transmission.
4) There are exactly two direct transmissions; one is by an STA and the other is by the AP back to the STA given that there is at least a direct transmission.

Therefore, P_s^{IBFD} is calculated based on the four cases of the conditional probabilities given above as follows

$$\begin{aligned}P_s^{IBFD} &= \frac{\tau_{AP}(1-\tau_{STA})^{n-1}}{P_{tr}^{IBFD}} \\ &\quad + \frac{(n-1)\tau_{STA}(1-\tau_{AP})(1-\tau_{STA})^{n-2}}{P_{tr}^{IBFD}} \\ &\quad + \frac{1}{n}\cdot\frac{1}{n-1}\cdot\frac{\tau_{AP}\tau_{STA}(1-\tau_{STA})^{n-2}}{P_{tr}^{IBFD}} \\ &\quad + \frac{n-1}{n}\cdot\frac{1}{n-1}\cdot\frac{\tau_{AP}\tau_{STA}(1-\tau_{STA})^{n-2}}{P_{tr}^{IBFD}} \\ &= \frac{\tau_{AP}(\overline{\tau}_{STA})^{n-1}}{P_{tr}^{IBFD}} \\ &\quad + \frac{(n-1)\tau_{STA}(\overline{\tau}_{AP})(\overline{\tau}_{STA})^{n-2}}{P_{tr}^{IBFD}} \end{aligned}$$

$$+\frac{1}{n(n-1)}\cdot\frac{\tau_{AP}\tau_{STA}(\overline{\tau}_{STA})^{n-2}}{P_{tr}^{IBFD}} + \frac{1}{n}\cdot\frac{\tau_{AP}\tau_{STA}(\overline{\tau}_{STA})^{n-2}}{P_{tr}^{IBFD}} \quad (51)$$

$$\Rightarrow P_s^{IBFD} = \frac{\tau_{AP}(\overline{\tau}_{STA})^{n-1} + (n-1)\tau_{STA}(\overline{\tau}_{AP})(\overline{\tau}_{STA})^{n-2}}{1-[(\overline{\tau}_{AP})(\overline{\tau}_{STA})^{n-1}]} + \frac{\tau_{AP}\tau_{STA}(\overline{\tau}_{STA})^{n-2}}{(n-1)\{1-[(\overline{\tau}_{AP})(\overline{\tau}_{STA})^{n-1}]\}} \quad (52)$$

using (54) for P_{tr}^{IBFD} from section VI-A.

When (52) is evaluated at $n = 2$, (52) becomes $P_s^{IBFD} = 1$ indicating that every transmission is successful, which is consistent with the result assuming $\tau_{AP} = \tau_{STA} = \tau$ reported in [34].

VI. IBFD-WLAN SYSTEM PERFORMANCE METRICS

In this section, IBFD-compatible metrics are outlined. The purpose of composing a portfolio of metrics is to measure the enhancements added by IBFD to WLAN performance. The metrics will be used to generate the results in Section VIII.

A. NETWORK THROUGHPUT

Throughput gain by IBFD was previously addressed in [34] where the focus there was primarily on presenting how collisions are treated and consequently affect the performance of normalized aggregate throughput. Therefore, the value of τ was directly obtained from [22]. The analysis in [34] is revisited here to include a more accurate model that considers both τ_{AP} and τ_{STA} derived in this paper. Additionally, the total network throughput is calculated in the absolute sense in terms of bits/second instead of the normalized value. Therefore, the *network throughput* can be expressed as

$$S^{IBFD} = \frac{P_s^{IBFD}P_{tr}^{IBFD}E[P](1+\Phi)}{\overline{P_{tr}^{IBFD}}\sigma + P_{tr}^{IBFD}P_s^{IBFD}T_s + P_{tr}^{IBFD}\overline{P_s^{IBFD}}T_c} \quad (53)$$

where the probability there is a transmission (P_{tr}^{IBFD}) is revised here to include both τ_{AP} and τ_{STA} as

$$P_{tr}^{IBFD} = 1-[(1-\tau_{AP})(1-\tau_{STA})^{n-1}] = 1-[(\overline{\tau}_{AP})(\overline{\tau}_{STA})^{n-1}]. \quad (54)$$

Note that

$$\overline{P_{tr}^{IBFD}} = 1 - P_{tr}^{IBFD} \quad (55)$$

and

$$\overline{P_s^{IBFD}} = 1 - P_s^{IBFD}. \quad (56)$$

Both T_s and T_c are reported respectively as (9) and (10) in section III. As explained in [34], since UL < DL, both the expected size of successfully transmitted MPDU and the expected size of a collision are equal to the load of the AP as follows

$$(E[P])^{IBFD} = (E[P^*])^{IBFD} = E[P_{AP}] = \text{MPDU}_{\max}. \quad (57)$$

B. FRAME AGGREGATION

Frame aggregation at the MAC sub-layer was introduced in the legacy IEEE 802.11n release [41] as a way to increase the efficiency of utilizing the channel by reducing the overhead. Aggregation enables an STA to concatenate several frames into a single transmission. As a result, the overhead is reduced since there is no need to allocate transmission time for more than a single header duration if the frames are combined into one transmission. Frame aggregation can be either Aggregated MAC Service Data Unit (A-MSDU) or Aggregated MPDU (A-MPDU). For the sake of this paper, MPDUs are aggregated. Details about frame aggregation in IEEE 802.11 standard can be found in [42] and [43].

The goal of frame aggregation in this paper is to increase traffic symmetry between UL and DL data loads and consequently serve traffic more efficiently. When frames are aggregated, the available IBFD UL transmission opportunity is utilized more efficiently since it is available until the *larger* DL transmission is finished. STAs can possibly aggregate frames to maximize the utilization of the established link with the AP. Increasing link utilization leads to increased network throughput because the amount of transmitted data increases. Moreover, when the number of transmitted frames increases due to aggregation, the average latency per frame decreases since more frames are pushed in the UL transmission opportunity.

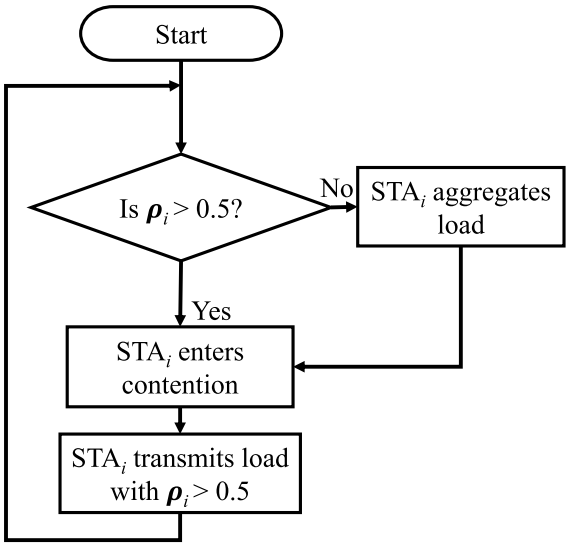

FIGURE 3. Flow chart of the proposed aggregation schemes.

This paper introduces two aggregation schemes which significantly improve network throughput, average latency, and link utilization. Fig. 3 shows a flow chart of how aggregation is performed based on the value of ρ at each STA. When an STA has $\rho > 0.5$, it cannot aggregate any more frames since the aggregated UL load would exceed the DL load, and the available transmission opportunity would not be sufficient to transmit the aggregated load before the AP finishes its DL transmission. On the contrary, when an STA has $\rho \leq 0.5$

and aggregates frames, the aggregated load can still be transmitted within the available transmission opportunity. The frame aggregation schemes proposed in this paper are namely *Dual-Frame Aggregation* and *Multi-Frame Aggregation*.

1) DUAL-FRAME AGGREGATION

In this aggregation scheme, any STA with $\rho \leq 0.5$ doubles its transmission load by aggregating two MPDUs. Thus,

$$\rho_{new}^{dual} := 2 \times \rho_{current}. \tag{58}$$

The *IBFD aggregation factor* (i.e., number of aggregated frames) for dual-frame aggregation is $\gamma^{dual} = 2$ if aggregation takes place. In this case, it is still guaranteed that each STA can fit its transmission while the IBFD connection is established with the AP since UL $\leq$ DL even after frame aggregation. Dual-frame aggregation increases the utilization of the available UL transmission time that would be otherwise not used.

2) MULTI-FRAME AGGREGATION

Some STAs with $\rho < 0.5$ can aggregate more than two frames in a transmission. The following is a simple rule to calculate IBFD aggregation factor for multi-frame aggregation in order to determine how many frames each STA can aggregate based on its current ρ value

$$\gamma^{multi} \triangleq \left\lfloor \frac{1}{\rho} \right\rfloor. \tag{59}$$

In this aggregation technique,

$$\rho_{new}^{multi} := \left\lfloor \frac{1}{\rho_{current}} \right\rfloor \times \rho_{current}. \tag{60}$$

The result of multi-frame aggregation is that STAs with very small ρ values can aggregate several frames, which increases both UL/DL traffic symmetry and utilization of available UL transmission time.

Dual-Frame Aggregation requires no calculations by STAs since the new load needs to simply be doubled if aggregation is possible. As for Multi-Frame Aggregation, determining the aggregated load either according to (60) above or by using a look-up table is required when aggregation takes place. For any STA with $\rho > 0.5$, no aggregation takes place ($\gamma^{dual} = \gamma^{multi} = 1$).

C. AVERAGE LATENCY

A similar analysis to the work in [35] is used to derive an analytical expression for average latency in IBFD-WLAN. According to [36], Little's Theorem classically states that the average number of customers in a system (N) is equal to the average arrival rate of the customers (λ) multiplied by the average delay per customer in the system (T). Thus,

$$N = \lambda T \Rightarrow T = \frac{N}{\lambda}. \tag{61}$$

Since saturated traffic is assumed in the network, the number of customers in the system is always equal to the number of nodes n. Unlike the case of HD latency considered in section III as (13), the case of IBFD transmission is more involved. The expected number of aggregated MPDUs, $E[\gamma]$, must be taken into consideration when calculating the frame arrival rate, which is equal to the frame departure rate since in a saturated buffer, a new (possibly aggregated) frame promptly arrives once the HOL frame is transmitted. Since one frame is transmitted in the DL direction and $E[\gamma]$ frames are transmitted in the UL direction, Little's Theorem can be applied to calculate the average latency per frame in an IBFD-WLAN as follows

$$\begin{aligned} D^{IBFD} &= \frac{n}{(1+E[\gamma]) \cdot S^{IBFD} \Big/ \Big[E[P_{AP}] \cdot (1+\Phi)\Big]} \\ &= \frac{n \cdot E[P_{AP}] \cdot (1+\Phi)}{(1+E[\gamma]) \cdot S^{IBFD}}. \end{aligned} \tag{62}$$

Every (aggregated) frame is ultimately delivered. This is true even in the case of a collision at the maximum backoff stage since the node resets to the initial backoff stage after the collision but keeps its load since the frame size is assumed to be constant for each node once assigned in a simulation run.

D. IBFD LINK UTILIZATION

Throughput quantifies successful transmission of data over the total time including successful transmission, collision, and sensing durations while considering added overhead. A metric that is worth introducing is IBFD link utilization, η, in order to quantify the efficiency of using the link (in both UL and DL directions) for transmission of useful data loads without the overhead. Since UL transmission is less than or equal to DL transmission, IBFD link utilization can be defined as

$$\eta \triangleq \frac{1+\Phi}{2} \times 100\%. \tag{63}$$

Ideally, if the channel is fully utilized in both UL and DL directions (i.e., $\rho = 1$ at each STA $\Rightarrow \Phi = 1$), then $\eta = 100\%$ indicating a fully utilized and symmetrical link. IBFD link utilization is particularly crucial when assessing the benefits of frame aggregation, and this becomes clear by the numerical results reported in Section VIII.

E. POWER CONSUMPTION

Power analysis is based on the classical definition of power (i.e., (14) in [37]). Therefore, a similar approach to the HD case reported in section III is adopted here to formulate a power consumption model for an IBFD-WLAN. Several factors are considered to account for an IBFD network. First, the AP properties in an IBFD system are different from those of STAs. Second, energy consumption for Self-Interference Cancellation (SIC) to enable IBFD communications must be added. Third, IBFD mechanisms must be factored into the expressions for each state.

1) THE AP IN AN INFRASTRUCTURE IBFD-WLAN

For the AP, there are 3 states as follows

1) Idle (AP-d)
2) Successful transmission/reception (AP-S-TXRX)
3) Transmitting/receiving a collision (AP-C-TXRX)

2) AN STA IN AN INFRASTRUCTURE IBFD-WLAN

For each STA, there are 5 states as follows

1) Idle (STA-d)
2) Successful transmission/reception (STA-S-TXRX)
3) Successful overhearing (STA-S-$\overline{\text{RX}}$)
4) Transmitting/receiving a collision (STA-C-TXRX)
5) Overhearing a collision (STA-C-$\overline{\text{RX}}$)

Based on the above considerations, the consumed energy and the probability of each state for the AP and an STA in an IBFD-WLAN are summarized below in (64) through (79). Then, energy and power calculations can be readily carried out in a similar way to the HD case given above by (27) and (28), respectively.

Energy Consumption for the AP in an infrastructure IBFD-WLAN:

$$\mathcal{E}_{\text{d}}^{\text{AP}} = \omega_{\text{d}}\sigma \tag{64}$$

$$\begin{aligned}\mathcal{E}_{\text{S-TXRX}}^{\text{AP}} &= \omega_{\text{TX+CTRL}}(\text{DATA}_{\text{TX}} + \text{ACK}) \\ &\quad + \omega_{\text{RX+SIC}}(\text{DATA}_{\text{RX}} + \text{ACK}) \\ &\quad + \omega_{\text{d}}(\text{DIFS} + \text{SIFS})\end{aligned} \tag{65}$$

$$\begin{aligned}\mathcal{E}_{\text{C-TXRX}}^{\text{AP}} &= \omega_{\text{TX+CTRL}}\text{DATA}_{\text{TX}} + \omega_{\text{RX+SIC}}\text{DATA}_{\text{RX}} \\ &\quad + \omega_{\text{d}}(\text{DIFS} + \text{SIFS} + \text{ACK})\end{aligned} \tag{66}$$

State Probabilities for the AP in an infrastructure IBFD-WLAN:

$$Pr(\text{AP-d}) = (1-\tau_{AP})(1-\tau_{STA})^{n-1} \tag{67}$$

$$\begin{aligned}Pr(\text{AP-S-TXRX}) &= \tau_{AP}(1-\tau_{STA})^{n-1} \\ &\quad + (n-1)\tau_{STA}(1-\tau_{STA})^{n-2}\end{aligned} \tag{68}$$

$$Pr(\text{AP-C-TXRX}) = 1 - Pr(\text{AP-d}) - Pr(\text{AP-S-TXRX}) \tag{69}$$

Energy Consumption for a STA in an infrastructure IBFD-WLAN:

$$\mathcal{E}_{\text{d}}^{\text{STA}} = \omega_{\text{d}}\sigma \tag{70}$$

$$\begin{aligned}\mathcal{E}_{\text{S-TXRX}}^{\text{STA}} &= \omega_{\text{TX+SIC}}(\text{DATA}_{\text{TX}} + \text{ACK}) \\ &\quad + \omega_{\text{RX+CTRL}}(\text{DATA}_{\text{RX}} + \text{ACK}) \\ &\quad + \omega_{\text{d}}(\text{DIFS} + \text{SIFS})\end{aligned} \tag{71}$$

$$\begin{aligned}\mathcal{E}_{\text{S-}\overline{\text{RX}}}^{\text{STA}} &= \omega_{\text{RX+CTRL}}(\text{DATA}_{\text{RX}} + \text{ACK}) \\ &\quad + \omega_{\text{d}}(\text{DIFS} + \text{SIFS})\end{aligned} \tag{72}$$

$$\begin{aligned}\mathcal{E}_{\text{C-TXRX}}^{\text{STA}} &= \omega_{\text{TX+SIC}}\text{DATA}_{\text{TX}} + \omega_{\text{RX+CTRL}}\text{DATA}_{\text{RX}} \\ &\quad + \omega_{\text{d}}(\text{DIFS} + \text{SIFS} + \text{ACK})\end{aligned} \tag{73}$$

$$\begin{aligned}\mathcal{E}_{\text{C-}\overline{\text{RX}}}^{\text{STA}} &= \omega_{\text{RX+CTRL}}\text{DATA}_{\text{RX}} \\ &\quad + \omega_{\text{d}}(\text{DIFS} + \text{SIFS} + \text{ACK})\end{aligned} \tag{74}$$

State Probabilities for an STA in an infrastructure IBFD-WLAN:

$$Pr(\text{STA-d}) = (1-\tau_{AP})(1-\tau_{STA})^{n-1} \tag{75}$$

$$Pr(\text{STA-S-TXRX}) = \tau_{STA}(1-p_{STA}) + (1-\tau_{STA})^{n-1}\frac{\tau_{AP}}{(n-1)} \tag{76}$$

$$\begin{aligned}Pr(\text{STA-S-}\overline{\text{RX}}) &= (n-2)\tau_{STA}(1-\tau_{STA})^{n-2}(1-\tau_{AP}) \\ &\quad + \frac{(n-2)}{(n-1)}\tau_{AP}\Big[\tau_{STA}(1-\tau_{STA})^{n-2} \\ &\quad + (1-\tau_{STA})^{n-1}\Big]\end{aligned} \tag{77}$$

$$Pr(\text{STA-C-TXRX}) = \tau_{STA}p_{STA} \tag{78}$$

$$\begin{aligned}Pr(\text{STA-C-}\overline{\text{RX}}) &= 1 - Pr(\text{STA-d}) - Pr(\text{STA-S-TXRX}) \\ &\quad - Pr(\text{STA-S-}\overline{\text{RX}}) \\ &\quad - Pr(\text{STA-C-TXRX})\end{aligned} \tag{79}$$

VII. DESCRIPTION OF IEEE 802.11 DCF SIMULATOR

In order to generate the simulation results presented in this paper, MATLAB was used to construct a discrete-event simulator. Actual parameters based on the latest IEEE 802.11ac standard [25] are used in the simulator, and key parameters are reported in TABLE 2. IEEE 802.11 DCF mechanisms are enforced to model how nodes behave in various states of idle channel, medium-access, collisions, and successful transmissions. Logs are used to record raw results such as sensing, collision, overhead, and successful transmission durations. System performance values such as throughput and latency are determined based on the raw results at the end of each simulation run. The simulator was constructed to be flexible when it comes to testing various network sizes and traffic loads. When random traffic scenarios are examined, a Monte Carlo simulation with 200 independent runs is used to ensure proper convergence to average results. The simulation results were verified by comparison with previously reported results in [22], [33], and [44], which were nearly identical.

The simulator was then extended to account for IBFD operations. Collisions were revisited in the simulator to ensure that IBFD collision treatment proposed in this paper is implemented. Collision lengths, successfully transmitted data, and overhead were revised to be compatible with IBFD operations. Frame aggregation schemes were also incorporated into the simulator, and calculating latency for IBFD-WLANs with aggregated traffic was properly handled. As reported in the next section, the simulation results closely match the calculated results using the analytical models reported in this paper.

VIII. RESULTS AND EVALUATION

In order to confirm the validity of the analytical model detailed in this paper for IBFD-WLAN, results based on simulated IEEE 802.11ac standard are used as a benchmark. Analytical and simulation results for both network throughput and average latency in standard HD IEEE 802.11, IBFD-WLAN, IBFD-WLAN with dual-frame aggregation,

and IBFD-WLAN with multi-frame aggregation are presented. In all generated results, the IBFD-WLAN analytical model provides values that closely match the simulated results within 1% error or less. Throughput quantifies successfully transmitted data over the total time. Latency quantifies the average time needed to successfully deliver an MPDU frame from the time the frame becomes HOL until an ACK frame is received. IBFD link utilization is used as a new metric to measure the enhancements added by IBFD aggregation techniques.

Both the IBFD-WLAN model proposed in this paper and the analytical model published in [21] are compared to simulated results. The performance of the network in terms of throughput, latency, and utilization when ρ values are deterministic is evaluated in order to illustrate the aggregation schemes and their benefits. The performance results are repeated when ρ values are random to show a more practical scenario for a typical network.

Power consumption and energy-efficiency are analyzed when the traffic is fully symmetrical (i.e., $\rho = 1$) for both HD and IBFD systems. The effect of symmetry on both power consumption and energy efficiency is presented through the two extreme cases of low symmetry ($\rho = 0.1$) and high symmetry ($\rho = 0.9$). The calculated power consumption values for ω_{TX}, ω_{RX}, and ω_d in TABLE 3 are based on [45]. Values of ω_{SIC} and ω_{CTRL} are stated in [46]. While ω_{SIC} accounts for both active and passive cancellation circuits, the majority of SIC is treated passively with minimal power consumption.

TABLE 3. Power consumption values.

Power Category	Value
Transmitter (ω_{TX})	2.6883 W
Receiver (ω_{RX})	1.5900 W
Idle State (ω_d)	0.9484 W
Control Circuit (ω_{CTRL})	0.3000 W
Self-Interference Cancellation (ω_{SIC})	0.0650 W

A. ACCURACY OF THE PROPOSED IBFD-WLAN MODEL

The reported graphs in [21] show noticeable discrepancies between simulation and analytical results for the performance of the network. Therefore, there is a need for an accurate analytical model that realizes the impact of IBFD on WLANs. Fig. 4 shows simulation results for network throughput versus number of nodes (n) in a WLAN based on IEEE 802.11 standard for three deterministic ρ values. The corresponding analytical results based on the IBFD-WLAN framework proposed in this paper are plotted. Additionally, the corresponding cases based on the analytical work reported in [21] are plotted for comparison. To make the comparison fair, the testing of the two analytical models was made closely similar by primarily using different formulas from the corresponding models for τ calculations while keeping all other parameters identical using the latest IEEE 802.11ac release (which [21] does not originally use). It is clear that at low n values, both analytical models match

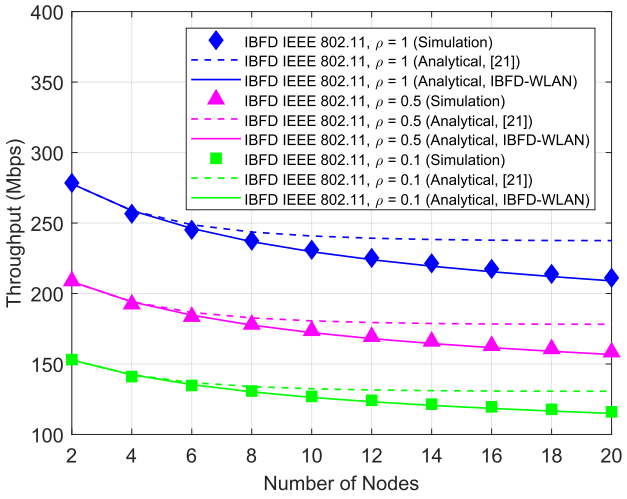

FIGURE 4. Comparison between throughput results from the proposed IBFD-WLAN analytical model and the analytical model published in [21].

the simulated results. However, at higher n values, the analytical model proposed in this paper continues to match the simulation results while the model from [21] provides overly optimistic results. For each curve, the average error between the simulated scenario and analytical results based on IBFD-WLAN model is always less than 1% (matching the accuracy of the well-studied HD IEEE 802.11 model). On the other hand, the mismatch introduced by [21] consistently increases as the number of nodes increases until it reaches about 13% in all three cases when $n = 20$. The high error at high n values cannot be justified by the fact that the model in [21] assumes, unlike IEEE 802.11 standard, infinite re-transmission attempts at the maximum backoff stage until the frame is successfully delivered. This difference alone can only provide much smaller deviation between simulation and analytical cases. The inaccurate results at high n values are also apparent in the reported plots in [21]. Latency comparison is not performed here since no complete analytical model for latency was reported in [21].

B. DETERMINISTIC ρ VALUES

Fig. 5 shows both analytical and simulation results for network throughput versus the number of nodes when each client STA always has $\rho = 0.3$ originally. The AP always transmits a load of $\text{MPDU}_{\max}$. The case for a standard HD IEEE 802.11 network is shown as a baseline case. When IBFD mode is enabled, the improvement in throughput depends on the number of nodes. For 2 nodes, the throughput increases by 72% compared to the case of HD IEEE 802.11 protocol. For 20 nodes, there is a 132% improvement in throughput when the IBFD mode is activated. The reason behind the difference in improvement is that the amount of transmitted data during each transmission opportunity in the HD mode is either $\text{MPDU}_{\max}$ (AP transmission) or $0.3 \times \text{MPDU}_{\max}$ (STA transmission). Therefore, when the number of nodes is high, there is less likelihood that the AP transmits its larger load, which yields significantly lower throughput in the HD mode.

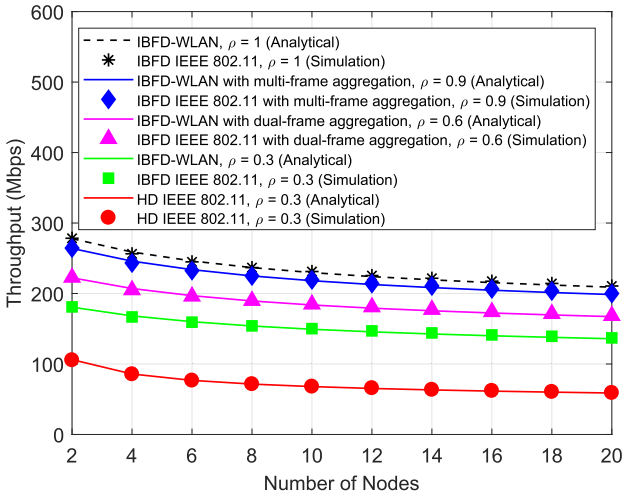

FIGURE 5. Throughput versus number of nodes ($\rho = 0.3$).

On the other hand, each transmission opportunity in the IBFD mode results in transmitting an $\text{MPDU}_{\max}$ in the DL direction *and* $0.3 \times \text{MPDU}_{\max}$ in the UL direction. When IBFD dual-frame aggregation is enabled, ρ_{new}^{dual} becomes 0.6. In this case, an increase of 23% is consistently realized in throughput compared to the case of IBFD without aggregation. The throughput is increased by 46% in each simulated case of n when IBFD multi-frame aggregation is employed in the network, which corresponds to $\rho_{new}^{multi} = 0.9$. The superior performance of IBFD multi-frame aggregation is expected since there is more data pushed in the UL direction. The upper limit for IBFD mode is indicated by the case when $\rho = 1$, and the increase in throughput from the case of IBFD without aggregation is 54%.

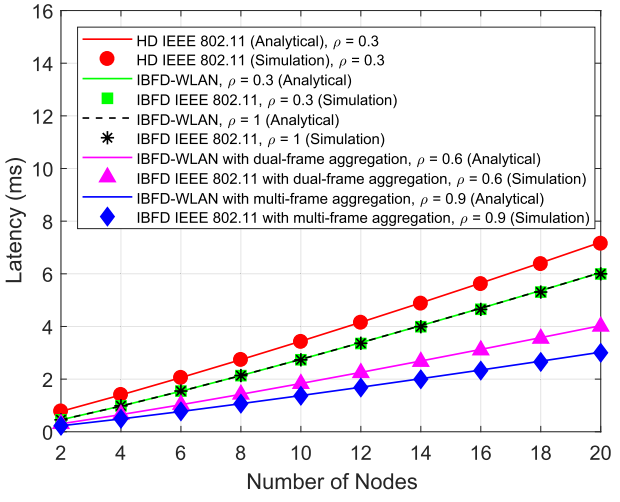

FIGURE 6. Latency versus number of nodes ($\rho = 0.3$).

Fig. 6 displays the results for latency versus n. HD IEEE 802.11 exhibits the highest latency since in each transmission opportunity, either a DL or a UL frame is transmitted. Once IBFD transmission is implemented, there is a reduction in latency since a DL frame *and* a UL frame are delivered in each transmission. When $n = 2$, there is a decrease of 42% in latency compared to HD IEEE 802.11. When n increases to 20, the reduction in latency is only 16% since there are more frames at silent STAs experiencing delay while an IBFD transmission takes place between the AP and an STA. The case for IBFD IEEE 802.11 with $\rho = 1$ (maximum traffic symmetry) is plotted. However, no further improvement in latency is realized since the number of delivered frames in each transmission is still 2. When IBFD IEEE 802.11 is augmented by dual-frame aggregation, there is a 33% improvement in latency for each case of n compared to IBFD without aggregation. The reason is that in each transmission, 1 DL frame and 2 UL frames are delivered. When multi-frame aggregation is introduced, latency is reduced by 50% compared to IBFD without aggregation since 1 DL frame and 3 UL frames are now served during each transmission. Clearly, aggregation is necessary to improve latency in IBFD-WLAN, and original ρ values do not affect average latency, which decreases as a result of increasing the number of transmitted frames.

Constant ρ values are assumed in this scenario, and the analytical values for η are as calculated in TABLE 4. The analytical results simply match the simulated results as expected since deterministic ρ values are assumed. It is worth noting that η is not affected by the number of nodes in the network since only the size of useful traffic is relevant here. The results for η indicate how well the channel is utilized in the assumed IBFD-WLAN network. IBFD link utilization becomes more sophisticated in the next sub-section for random ρ values.

TABLE 4. IBFD link utilization for deterministic ρ values.

Aggregation Mode	$\rho_{original}$	γ	ρ_{new}	Φ	η
Pure IBFD (no aggregation)	0.3	1	0.3	0.3	65%
IBFD dual-frame aggregation	0.3	2	0.6	0.6	80%
IBFD multi-frame aggregation	0.3	3	0.9	0.9	95%

C. RANDOM ρ VALUES

In this section, a ρ value for each client STA is randomly assigned such that ρ is uniformly distributed over $\{0.1, 0.2, \ldots, 0.9\}$. New ρ assignments are updated in each simulation run. The average result of 200 independent runs is reported for each simulation scenario. For IBFD dual-frame aggregation, only STAs with $0.1 \leq \rho \leq 0.5$ double their loads while the rest of STAs with $0.6 \leq \rho \leq 0.9$ maintain their original frames. When IBFD multi-frame aggregation is used, STAs with $0.6 \leq \rho \leq 0.9$ transmit their original loads while the rest of STAs aggregate their loads according to TABLE 5, which shows aggregation rules for both dual-frame and multi-frame modes. Fig. 7 shows throughput results versus n. When $n = 2$, IBFD introduces an 85% increase in throughput compared to 112% increase when $n = 20$ (both comparisons are with the corresponding HD cases). The difference in improvement between the two cases is consistent with the case of deterministic ρ values in section VIII-B in

TABLE 5. IBFD frame aggregation rules for random ρ values.

$\rho_{current}$	Dual-Frame		Multi-Frame	
	γ	ρ_{new}	γ	ρ_{new}
0.1	2	0.2	10	1
0.2	2	0.4	5	1
0.3	2	0.6	3	0.9
0.4	2	0.8	2	0.8
0.5	2	1	2	1
0.6	1	0.6	1	0.6
0.7	1	0.7	1	0.7
0.8	1	0.8	1	0.8
0.9	1	0.9	1	0.9

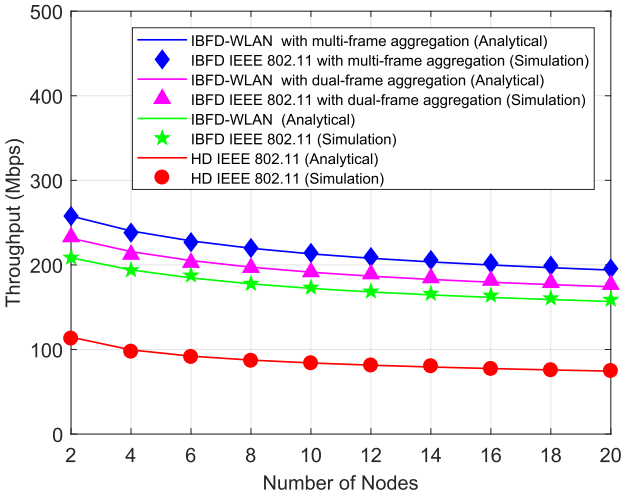

FIGURE 7. Throughput versus number of nodes (random ρ values, 200 runs).

that there is much less data transmitted in the DL direction when n is high resulting in low throughput in the HD baseline case. When dual-frame aggregation is employed, there is an improvement of 11% in throughput for each case of n compared to the corresponding IBFD case without aggregation. For multi-frame aggregation, the increase in throughput is 24%. Thus, IBFD multi-frame aggregation provides superior performance as expected since more UL transmission time is utilized.

Fig. 8 displays latency results versus n when ρ values are random. IBFD without aggregation reduces latency by 45% compared to the HD case when $n = 2$, but the improvement in latency decreases as the number of nodes increases until it reaches 33% when $n = 12$. Even though increasing the number of nodes increases latency as expected, improvement in latency due to IBFD transmission remains unaffected and stays at 33% as n increases. This behavior is consistent with the scenario of deterministic ρ values in that as n continues to increase, nodes in the HD network experience higher delays while waiting for the active transmission to finish. Dual-frame aggregation introduces 16% of reduction in latency when $n = 2$ compared to IBFD without aggregation, and the improvement saturates to 22% as n increases. Multi-frame aggregation initially introduces 31% improvement when $n = 2$ compared to IBFD without aggregation, and the improvement saturates to 47% for higher values of n. In both aggregation schemes, more reduction

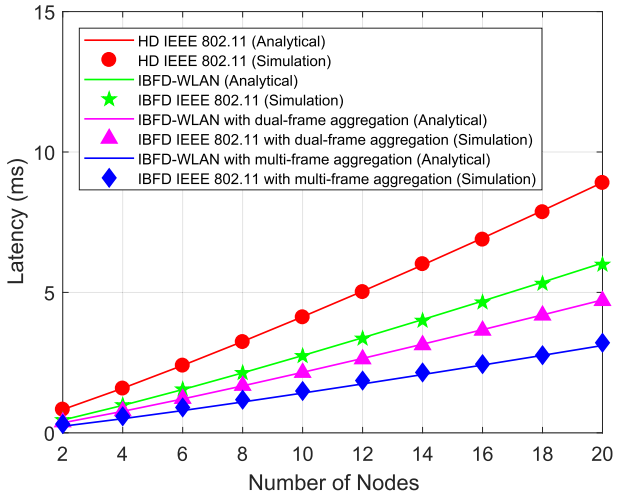

FIGURE 8. Latency versus number of nodes (random ρ values, 200 runs).

in latency is noted as n increases. This behavior can be explained by the fact that as the number of nodes increases, there are more STAs that can initially have low ρ values, which enable them to aggregate and transmit more frames. Therefore, the expected total number of transmitted frames in the UL direction increases as n increases, which further reduces the average latency.

Since the value of ρ is equally likely to be one of the uniformly distributed values between 0.1 and 0.9, $E[\gamma]$ can be directly calculated based on the values in TABLE 5. In addition, analytical values for η in the case of random ρ values are readily obtained based on the calculated values of Φ, and the results are summarized in TABLE 6. Average simulation results from 200 runs are also reported for $E[\gamma]$, Φ, and η. It is noted that the values of η are directly proportional to the values of Φ as expected. When random ρ values are introduced into the system, simulation results for IBFD performance metrics are in strong agreement with the analytical results and still consistent with the case of deterministic ρ values.

TABLE 6. IBFD link utilization for random ρ values.

Aggregation Mode	Analytical			Simulation		
	$E[\gamma]$	Φ	η	$E[\gamma]$	Φ	η
None	1	0.5000	75.00%	1	0.5044	75.22%
Dual-frame	1.5556	0.6667	83.34%	1.5608	0.6649	83.24%
Multi-frame	2.8889	0.8556	92.78%	2.8915	0.8545	92.72%

D. FULLY SYMMETRICAL TRAFFIC

Fig. 9 shows how the number of nodes affects the power consumption per node in both HD and IBFD networks. Both analytical and simulation results are reported when the traffic is assumed to be fully symmetrical. This is the best case scenario where the link is fully utilized in both uplink and downlink directions. In the HD case, the AP and every STA have identical power consumption since HD IEEE 802.11 yields the same power profile for every node. The power consumption per node in an HD WLAN stabilizes at a constant value

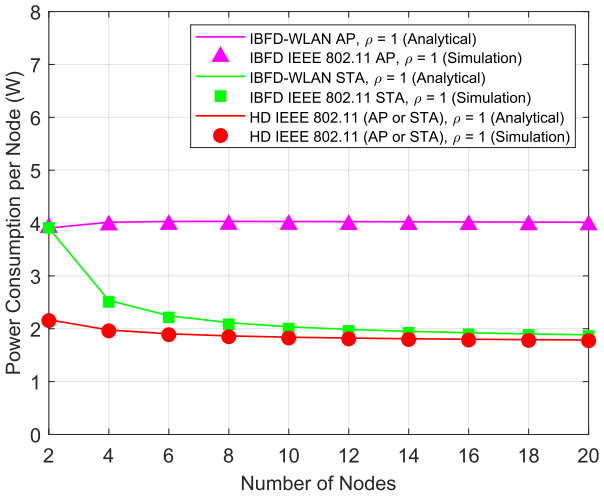

FIGURE 9. Power consumption per node in HD and IBFD-WLANs when $\rho = 1$.

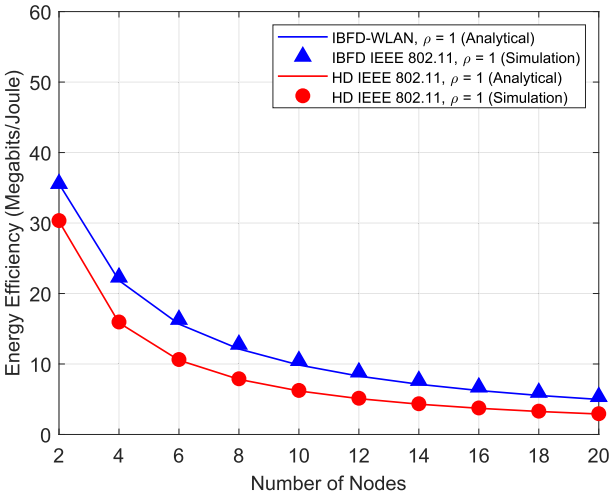

FIGURE 10. Energy-efficiency in HD and IBFD-WLANs when $\rho = 1$.

as the number of nodes increases since the dominant power consumption mode happens in states S-TX and C-TX, and the associated probabilities for both transmitting states reach a steady value quickly as the number of nodes increases. In the case of IBFD-WLAN, the results are reported for both the AP and an STA since they have different properties here. Power consumption is higher in IBFD-WLANs since there is simultaneous transmission and reception at both the AP and an STA when the channel is non-idle. The AP in an IBFD-WLAN has high power consumption since it is always transmitting (states AP-S-TXRX and AP-C-TXRX) regardless of how many STAs are in the network. This does not constitute an efficiency concern since APs are typically powered by AC electricity in residential WLANs. As the number of nodes increases, power consumption per STA gradually decreases to reach a constant value since the probability values of transmitting states (i.e., STA-S-TXRX and STA-C-TXRX) quickly stabilize as the number of nodes becomes high. When $n = 2$ with fully symmetrical traffic loads, the AP and the STA have the same power consumption in the IBFD case since they have the same probabilistic properties with no collision and no overhearing from either nodes as indicated in [34].

Fig. 10 shows analytical and simulation results of energy-efficiency in terms of Megabits/Joule resulting from dividing throughput by consumed power as in [46]. The results are reported for both HD and IBFD cases. IBFD-WLANs always have higher energy-efficiency since more data is transmitted. A key reason here is that only one node uses the link for data transmission in HD networks while two transmitting nodes utilize the link for data transmission in an IBFD-WLAN.

E. HIGH SYMMETRY VS. LOW SYMMETRY

Fig. 11 shows the results of power consumption per node in both HD and IBFD-WLANs. High symmetry ($\rho = 0.9$) and low symmetry ($\rho = 0.1$) are considered. Similar patterns to

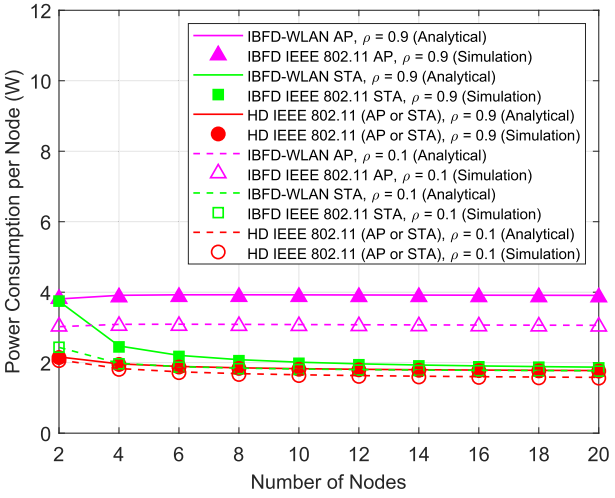

FIGURE 11. Power consumption per node in HD and IBFD-WLANs.

the ones in Fig. 9 can be seen here. Power consumption is reduced when symmetry is low since lower power consumption is needed to transmit (and receive) smaller uplink traffic loads. For HD WLAN, the power consumption is slightly affected by the change of symmetry mode but remains lower than the corresponding IBFD case. In the special case when an IBFD-WLAN has two nodes, the network becomes more efficient due to the elimination of collisions [34]. In this case, the STA has higher power consumption than the corresponding HD case since it is simultaneously transmitting and receiving with IBFD. Power consumption increases as symmetry increases because more power is needed to transmit a larger uplink payload. The power consumption of the AP in the IBFD case with $n = 2$ increases when the uplink load increases due to the increase in power consumption at the AP's receiver.

Fig. 12 shows the energy-efficiency for the cases of high and low symmetry scenarios in both HD and IBFD-WLANs. The key result in this figure is that energy-efficiency

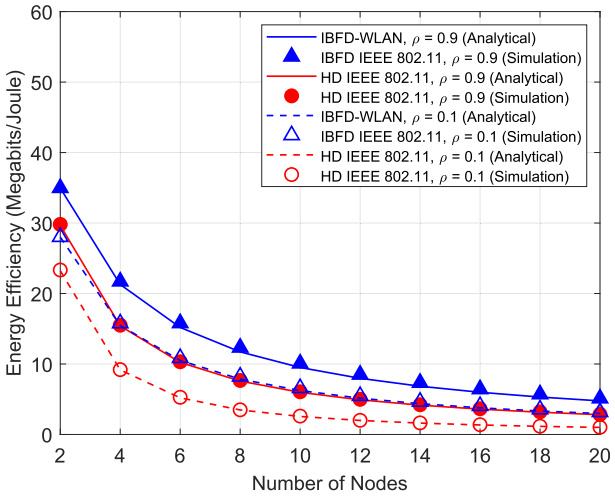

FIGURE 12. Energy-efficiency in HD and IBFD-WLANs.

of low symmetry IBFD-WLAN is almost equal to the energy-efficiency of high symmetry HD WLAN. The low symmetry scenario is naturally inefficient due to the lower utilization of the uplink. Hence, it takes an extremely inefficient assumption (i.e., low symmetry) to reduce the high efficiency of an IBFD-WLAN to the upper limit of energy-efficiency in the HD case. This result is intuitive since an IBFD-WLAN with low symmetry has effectively only one fully utilized communications direction (i.e., downlink), which is equivalent to the fully utilized communications direction (i.e., either the uplink or downlink) in the HD WLAN with high symmetry. When $n = 2$, the increase of energy-efficiency as the symmetry increases is due to the higher data amount transmitted over the link. Even though more power is needed when there is a larger data load, both HD and IBFD networks show increase in efficiency when the traffic is highly symmetrical. The increase of efficiency in an IBFD-WLAN as symmetry increases shows that the increase of transmitted data is high enough to overcome the increase in consumed power.

IX. CONCLUSION

In this paper, an accurate model characterizing IEEE 802.11 DCF for IBFD-WLAN is presented. The model is based on a two-dimensional DTMC framework. The concepts of IBFD transmission and frame aggregation are combined to maximize throughput and minimize latency in WLANs. The proposed aggregation schemes increase the utilization of available UL transmission time that would otherwise be unused. Each client STA uses its own traffic information to make a localized decision about the option and size of aggregation. Aggregation is necessary to minimize latency in IBFD-WLANs. The proposed analytical model and related metrics are robust and produce values coinciding with the simulated results even when randomness is introduced in the system. Since no changes to IEEE 802.11 protocol were introduced in this paper, the proposed IBFD frame aggregation schemes would be backward compatible with future IEEE 802.11 releases (e.g., IEEE 802.11ax). Even though power consumption is higher in IBFD-WLANs compared to HD WLANs, IBFD networks still have higher energy-efficiency. Network throughput, average latency, link utilization, and energy-efficiency are proposed as metrics to quantify potential enhancements resulting from introducing IBFD in WLANs. Future work can consider fairness analysis, hidden terminals, unsaturated traffic buffers, and exact treatment for decoding MAC headers.

REFERENCES

[1] *The Zettabyte Era: Trends and Analysis*, Cisco, San Jose, CA, USA, Jun. 2017.
[2] *Cisco Visual Networking Index*, Cisco, San Jose, CA, USA, Feb. 2017.
[3] *Wireless LAN Medium Access Control (MAC) and Physical Layer (PHY) Specifications*, IEEE Standard 802.11, 2012.
[4] A. Sabharwal, P. Schniter, D. Guo, D. W. Bliss, S. Rangarajan, and R. Wichman, "In-band full-duplex wireless: Challenges and opportunities," *IEEE J. Sel. Areas Commun.*, vol. 32, no. 9, pp. 1637–1652, Sep. 2014.
[5] D. Kim, H. Lee, and D. Hong, "A survey of in-band full-duplex transmission: From the perspective of PHY and MAC layers," *IEEE Commun. Surveys Tuts.*, vol. 17, no. 4, pp. 2017–2046, Feb. 2015.
[6] Z. Zhang, K. Long, A. V. Vasilakos, and L. Hanzo, "Full-duplex wireless communications: Challenges, solutions, and future research directions," *Proc. IEEE*, vol. 104, no. 7, pp. 1369–1409, Jul. 2016.
[7] S. Katti, "Full duplex radios," in *Proc. ACM SIGCOMM Conf.*, Hong Kong, 2013, pp. 375–386.
[8] E. Ahmed, A. M. Eltawil, and A. Sabharwal, "Self-interference cancellation with nonlinear distortion suppression for full-duplex systems," in *Proc. Asilomar Conf. Signals, Syst. Comput.*, Nov. 2013, pp. 1199–1203.
[9] E. Ahmed and A. M. Eltawil, "All-digital self-interference cancellation technique for full-duplex systems," *IEEE Trans. Wireless Commun.*, vol. 14, no. 7, pp. 3519–3532, Jul. 2015.
[10] M. Duarte, C. Dick, and A. Sabharwal, "Experiment-driven characterization of full-duplex wireless systems," *IEEE Trans. Wireless Commun.*, vol. 11, no. 12, pp. 4296–4307, Dec. 2012.
[11] E. Ahmed, A. M. Eltawil, Z. Li, and B. A. Cetiner, "Full-duplex systems using multireconfigurable antennas," *IEEE Trans. Wireless Commun.*, vol. 14, no. 11, pp. 5971–5983, Nov. 2015.
[12] M. Duarte, A. Sabharwal, V. Aggarwal, R. Jana, K. K. Ramakrishnan, C. W. Rice, and N. K. Shankaranarayanan, "Design and characterization of a full-duplex multiantenna system for WiFi networks," *IEEE Trans. Veh. Technol.*, vol. 63, no. 3, pp. 1160–1177, Mar. 2014.
[13] M. Jain, J. I. Choi, T. Kim, D. Bharadia, S. Seth, K. Srinivasan, P. Levis, S. Katti, and P. Sinha, "Practical, real-time, full duplex wireless," in *Proc. 17th Annu. Int. Conf. Mobile Comput. Netw. (MobiCom)*, New York, NY, USA, 2011, pp. 301–312.
[14] M. Luvisotto, A. Sadeghi, F. Lahouti, S. Vitturi, and M. Zorzi, "RCFD: A novel channel access scheme for full-duplex wireless networks based on contention in time and frequency domains," *IEEE Trans. Mobile Comput.*, vol. 17, no. 10, pp. 2381–2395, Oct. 2018.
[15] H. Zuo, Y. Sun, S. Li, Q. Cao, Y. Chen, W. Shi, and X. Wang, "A distributed IBFD MAC mechanism and non-saturation throughput analysis for wireless networks," in *Proc. 13th Int. Wireless Commun. Mobile Comput. Conf. (IWCMC)*, Jun. 2017, pp. 1851–1856.
[16] R. Doost-Mohammady, M. Y. Naderi, and K. R. Chowdhury, "Performance analysis of CSMA/CA based medium access in full duplex wireless communications," *IEEE Trans. Mobile Comput.*, vol. 15, no. 6, pp. 1457–1470, Jun. 2016.
[17] Y. Liao, K. Bian, L. Song, and Z. Han, "Full-duplex MAC protocol design and analysis," *IEEE Commun. Lett.*, vol. 19, no. 7, pp. 1185–1188, Jul. 2015.
[18] D. Marlali and O. Gurbuz, "Design and performance analysis of a full-duplex MAC protocol for wireless local area networks," *Ad Hoc Netw.*, vol. 67, pp. 53–67, Dec. 2017.
[19] E. Askari and S. Aïssa, "Single-band full-duplex MAC protocol for distributed access networks," *IET Commun.*, vol. 8, no. 10, pp. 1663–1673, Jul. 2014.

[20] A. Tang and X. Wang, "A-duplex: Medium access control for efficient coexistence between full-duplex and half-duplex communications," *IEEE Trans. Wireless Commun.*, vol. 14, no. 10, pp. 5871–5885, Oct. 2015.
[21] K.-H. Lee and J. Yoo, "Performance of the full-duplex MAC protocol in non-saturated conditions," *IEEE Commun. Lett.*, vol. 21, no. 8, pp. 1827–1830, Aug. 2017.
[22] G. Bianchi, "Performance analysis of the IEEE 802.11 distributed coordination function," *IEEE J. Sel. Areas Commun.*, vol. 18, no. 3, pp. 535–547, Mar. 2000.
[23] C. Chen, S. Hou, and S. Wu, "Saturation throughput analysis of an asymmetric full-duplex MAC protocol in WLANs with hidden terminals," *IEEE Access*, vol. 6, pp. 69948–69960, 2018.
[24] K. Sanada and K. Mori, "Throughput analysis for full duplex wireless local area networks with hidden nodes," in *Proc. 16th IEEE Annu. Consum. Commun. Netw. Conf. (CCNC)*, Jan. 2019, pp. 1–4.
[25] *Wireless LAN Medium Access Control (MAC) and Physical Layer (PHY) Specifications: Enhancements for Very High Throughput for Operation in Bands Below 6 GHz*, IEEE Standard 802.11ac, 2013.
[26] N. Iida, T. Nishio, M. Morikura, K. Yamamoto, T. Nabetanit, and T. Aoki, "Frame length optimization for in-band full-duplex wireless LANs," in *Proc. 21st Asia–Pacific Conf. Commun. (APCC)*, Oct. 2015, pp. 354–358.
[27] J. Hu, B. Di, Y. Liao, K. Bian, and L. Song, "Hybrid MAC protocol design and optimization for full duplex Wi-Fi networks," *IEEE Trans. Wireless Commun.*, vol. 17, no. 6, pp. 3615–3630, Jun. 2018.
[28] H. Zuo, Y. Sun, S. Li, Q. Cao, H. Xu, and G. Zhou, "A distributed medium access mechanism for in-band full-duplex wireless networks," in *Proc. Int. Wireless Commun. Mobile Comput. Conf. (IWCMC)*, Sep. 2016, pp. 958–963.
[29] H. J. Yang, H. W. Park, and H. Jin, "Performance analysis of infrastructure WLANs with multi-packet reception and full-duplex radio," in *Proc. Int. Conf. Inf. Commun. Technol. Converg. (ICTC)*, Oct. 2015, pp. 1307–1311.
[30] Y. Liao, B. Di, K. Bian, L. Song, D. Niyato, and Z. Han, "Cross-layer protocol design for distributed full-duplex network," in *Proc. IEEE Global Commun. Conf. (GLOBECOM)*, Dec. 2015, pp. 1–6.
[31] R. Liao, B. Bellalta, and M. Oliver, "Modelling and enhancing full-duplex MAC for single-hop 802.11 wireless networks," *IEEE Wireless Commun. Lett.*, vol. 4, no. 4, pp. 349–352, Aug. 2015.
[32] M. Hirzallah, W. Afifi, and M. Krunz, "Provisioning QoS in Wi-Fi systems with asymmetric full-duplex communications," *IEEE Trans. Cognit. Commun. Netw.*, vol. 4, no. 4, pp. 942–953, Dec. 2018.
[33] I. Tinnirello, G. Bianchi, and Y. Xiao, "Refinements on IEEE 802.11 distributed coordination function modeling approaches," *IEEE Trans. Veh. Technol.*, vol. 59, no. 3, pp. 1055–1067, Mar. 2010.
[34] M. Murad and A. M. Eltawil, "Collision tolerance and throughput gain in full-duplex IEEE 802.11 DCF," in *Proc. IEEE Int. Conf. Commun. (ICC)*, May 2018, pp. 1–6.
[35] G. Bianchi, S. Choi, and I. Tinnirello, "Performance study of IEEE 802.11 DCF and IEEE 802.11 e EDCA," in *Emerging Technologies in Wireless LANs: Theory, Design, and Deployment*, B. Bing, Ed. New York, NY, USA: Cambridge Univ. Press, 2008, ch. 4, p. 83.
[36] D. P. Bertsekas and R. G. Gallager, *Data Networks*. Upper Saddle River, NJ, USA: Prentice-Hall, 1992.
[37] C. K. Alexander and M. N. O. Sadiku, *Fundamentals of Electric Circuits*. New York, NY, USA: McGraw-Hill, 2017.
[38] M. Ergen and P. Varaiya, "Decomposition of energy consumption in IEEE 802.11," in *Proc. IEEE Int. Conf. Commun.*, Jun. 2007, pp. 403–408.
[39] M. Murad and A. M. Eltawil, "A simple full-duplex MAC protocol exploiting asymmetric traffic loads in WiFi systems," in *Proc. IEEE Wireless Commun. Netw. Conf. (WCNC)*, Mar. 2017, pp. 1–6.
[40] W. Choi, H. Lim, and A. Sabharwal, "Power-controlled medium access control protocol for full-duplex WiFi networks," *IEEE Trans. Wireless Commun.*, vol. 14, no. 7, pp. 3601–3613, Jul. 2015.
[41] *Wireless LAN Medium Access Control (MAC) and Physical Layer (PHY) Specifications: Enhancements for Higher Throughput*, IEEE Standatd 802.11n, 2009.
[42] R. Karmakar, S. Chattopadhyay, and S. Chakraborty, "Impact of IEEE 802.11n/ac PHY/MAC high throughput enhancements on transport and application protocols—A survey," *IEEE Commun. Surveys Tuts.*, vol. 19, no. 4, pp. 2050–2091, 2017.
[43] E. Perahia and R. Stacey, *Next Generation Wireless LANs: 802.11n and 802.11ac*. New York, NY, USA: Cambridge Univ. Press, 2013.
[44] P. Chatzimisios, A. C. Boucouvalas, and V. Vitsas, "IEEE 802.11 packet delay—A finite retry limit analysis," in *Proc. IEEE Global Telecommun. Conf. (GLOBECOM)*, vol. 2, Dec. 2003, pp. 950–954.
[45] O. Lee, J. Kim, and S. Choi, "WiZizz: Energy efficient bandwidth management in IEEE 802.11ac wireless networks," in *Proc. 12th Annu. IEEE Int. Conf. Sens., Commun., Netw. (SECON)*, Jun. 2015, pp. 136–144.
[46] M. Kobayashi, R. Murakami, K. Kizaki, S. Saruwatari, and T. Watanabe, "Wireless full-duplex medium access control for enhancing energy efficiency," *IEEE Trans. Green Commun. Netw.*, vol. 2, no. 1, pp. 205–221, Mar. 2018.

MURAD MURAD (Member, IEEE) received the B.Sc. degree *(summa cum laude)* in electrical engineering from California State University, Long Beach (CSULB), the M.E. degree in electrical engineering from The University of British Columbia (UBC), Vancouver, Canada, and the Ph.D. degree in electrical engineering from the University of California Irvine (UCI).

He is a Research Associate with the Wireless Systems and Circuits Laboratory, UCI, where he pursued original contributions to achieve cutting-edge results in improving the design of wireless networks based on in-band full-duplex techniques. He is currently the Director of Technology Research Department with the Ministry of Communications and Information Technology, Saudi Arabia, where he leads both technology scanning and future foresight functions. He previously worked at Saudi Aramco, as an Information Technology Professional, handling both managerial and technical responsibilities. He led teams to run daily telecommunications and data networking operations. He also worked as a Communications Engineer, handling communications systems and projects in this field. He received training on various communications and networking systems from leading vendors in the industry.

AHMED M. ELTAWIL (Senior Member, IEEE) received the B.Sc. and M.Sc. degrees (Hons.) from Cairo University, Giza, Egypt, in 1997 and 1999, respectively, and the Ph.D. degree from the University of California at Los Angeles, in 2003. Since 2005, he has been with the Department of Electrical Engineering and Computer Science, University of California Irvine, where he was the Founder and the Director of the Wireless Systems and Circuits Laboratory. Since 2019, he has been a Professor with the Computer, Electrical, and Mathematical Science and Engineering Division (CEMSE), King Abdullah University of Science and Technology (KAUST), Thuwal, Saudi Arabia. His research interests include low-power digital circuits and signal processing architectures with an emphasis on mobile systems. He received several awards as well as distinguished grants, including the NSF CAREER Grant, supporting his research in low-power systems. He has been serving on the technical program committees and steering committees for numerous workshops, symposia, and conferences in the areas of low power computing and wireless communication system design.